DETAILED MEASUREMENTS OF ROOM AIR DISTRIBUTION FOR EVALUATING NUMERICAL SIMULATION MODELS

J.S. Zhang, Ph.D.
Associate Member ASHRAE

L.L. Christianson, Ph.D., P.E.
Member ASHRAE

G.J. Wu, P.E.
Member ASHRAE

G.L. Riskowski, Ph.D., P.E.

ABSTRACT

Two-dimensional isothermal and non-isothermal airflows were measured in a full-scale room (24 ft × 18 ft × 8 ft). Measurements included the flow patterns of the room air, the profiles of air velocity and turbulent kinetic energy at the diffuser, and velocities, turbulent kinetic energies, and temperatures at 205 locations within the room. The measurement grid was non-uniform, with higher grid density in flow regions where relatively high velocity gradients were expected (e.g., the diffuser jet region). The data show the effects of sampling rates and sampling periods on the experimental results, the effects of internal heat load on the airflow pattern, as well as the difference between the diffuser jet region and the occupied region in terms of turbulent kinetic energy and power spectrums. Such detailed measurements are useful for evaluating numerical simulation models as well as for understanding the behavior of the room ventilation airflows.

INTRODUCTION

Evaluating and improving numerical models of room air distribution require detailed measurements of air velocity, temperature, and turbulence characteristics. Current data are insufficient for numerical modelers because more data are needed for realistic low-turbulence ventilation flows and profiles of velocity and turbulent kinetic energy at the diffuser and the boundary layer over solid surfaces within the room. The recent symposium "Building Systems: Room Air and Air Contaminant Distribution" (Christianson 1989) identified the need for these data and their application to the numerical models as two of the six primary research needs in this field.

Much of the detailed room air movement data available are from research in the 1950s through 1970s (Straub and Chen 1957; Miller and Nash 1971). Those data are valuable and have provided design guidelines for space air diffusion (ASHRAE 1989). Their instrumentation was not designed to measure the turbulence characteristics, so the turbulence features of the flow were not reported.

Air diffuser manufacturers have also studied room air movement characteristics in full and part scale for many alternative diffuser designs and room designs (e.g., Hart and Int-Hout 1980 and Lorch and Straub 1983). These data help engineers select diffusers appropriate for specific applications. However, these data are also limited in detail, especially at the diffuser and at the boundary layers.

Many researchers have measured air velocities in reduced-scale rooms and used similitude theory to interpret the results (e.g., Nielsen 1989; Timmons 1979; Murakami and Kato 1989; Zhang et al. 1989). However, most experiments were limited to fully developed flow conditions, which are not common in typical commercial and residential rooms. Moreover, the turbulence characteristics were not measured in most of these studies.

Hanzawa et al. (1987) and Sandberg (1989) measured air velocities and turbulence characteristics in full-scale rooms. These data are valuable for understanding the turbulent characteristics of the room ventilation flows, but the spatial distribution of the velocity and turbulent kinetic energy was not reported.

The objectives of the research reported in this paper were to (1) provide detailed experimental data for evaluating numerical simulation models and (2) improve the understanding of the turbulent characteristics of room ventilation flow, which is essential for improving existing numerical models and for developing new models.

FACILITY AND PROCEDURES

A room ventilation simulator has been developed for studying room air and air contaminant movement within ventilated rooms. It has an inner testing room and an outer room for controlling the ambient air condition of the inner room (Figure 1). Alternatively, air can be conditioned independent of the outer room condition and

Jianshun S. Zhang is a research engineer, **Leslie L. Christianson** is a professor, **G. Jeff Wu** is a research associate, and **Gerald L. Riskowski** is an assistant professor in agricultural engineering at the University of Illinois, Urbana-Champaign.

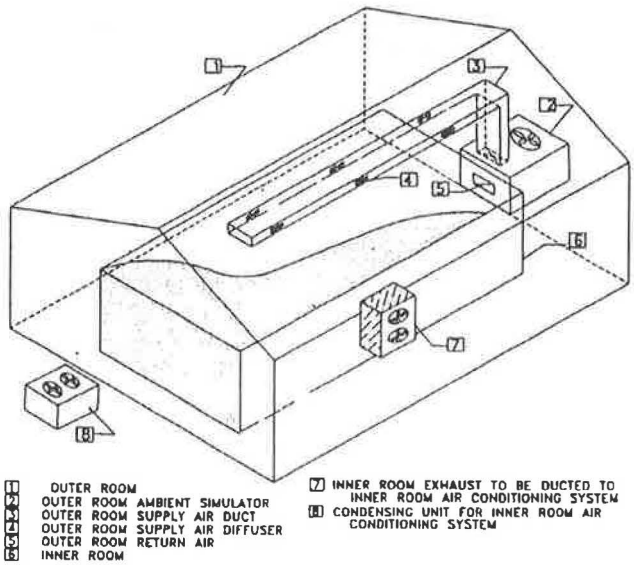

Figure 1 *Schematic of the room ventilation simulator.*

supplied to the inner test room. The inner room is designed on a modular basis so different room configurations and sizes can be investigated. Details of the room ventilation simulator are described by Wu et al. (1990).

The experimental arrangements for the present full-scale tests consist of a test room (24 ft × 18 ft × 8 ft), an exhaust plenum (24 ft × 10 ft × 8 ft), an air delivery chamber, a centrifugal fan, and a probe traverse unit (Figure 2). Since the test room has a continuous slot diffuser and a continuous slot exhaust opening, the flow within the room is practically two dimensional (Zhang 1991). For non-isothermal tests, 48 electrical heating panels (4 ft × 2 ft) are uniformly arranged on the floor to provide the internal heat load from 0 to 56 Btu/(h·ft^2) (178 W/m^2). The test room and the exhaust plenum chamber are well insulated so that heat loss through the walls, ceiling, and floor is negligible (Zhang 1991).

The velocities and temperatures within the room are measured with a hot wire probe and a thermocouple probe, respectively. Both probes are mounted on the traverse unit. A microcomputer-based data acquisition and probe-positioning system has been developed to collect the data and move the probes automatically (Figure 3).

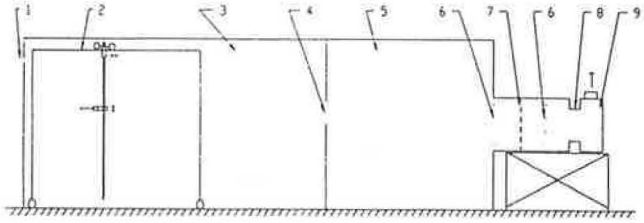

Figure 2 *Experimental setup for the full-scale room.*

TABLE 1
Experimental Conditions*

Test	U_d (ft/min)	T_d (°F)	T_e (°F)	T_f (°F)	ΔT_{fd} (°F)	Re_d	Ar_{fd}	Q (ach)
1	350	75	75	75	0	5735	0	19.5
2	350	75.4	90.3	142.7	67.3	5735	0.0186	19.5

*All variables are defined in the nomenclature section.

Additionally, the temperatures at the diffuser, exhaust of the test room, and the floor surface are monitored by a separate data logger with thermocouple.

Two sets of data are presented in the present study (Table 1), in which velocities and temperatures were measured at 205 locations along the central section of the test room and at the diffuser (Figure 4). The hot wire probe was oriented so that the sensing wire was perpendicular to the two-dimensional flow plan to minimize the effect of the third velocity component. Additionally, the airflow patterns within the room were visualized by injecting titanium tetrachloride smoke at different locations.

RESULTS AND DISCUSSION[1]

Sampling Rate and Sampling Period

The sampling rate of velocity measurements needs to be sufficiently high so that the high-frequency fluctuations in the airflow can be captured. A representative velocity sample in the diffuser jet region is shown in Figure 5. Sampling with 250 Hz captured 95% of the velocity fluctuations. This sampling frequency would also be suitable for the other parts of the room, since the velocity fluctuations there would contain lower frequency components due to the lower mean velocity gradients as compared to the diffuser jet region. According to Nyquist sampling theorem (Bendat and Piersol 1986), with such a sampling rate, we will be able to calculate the energy

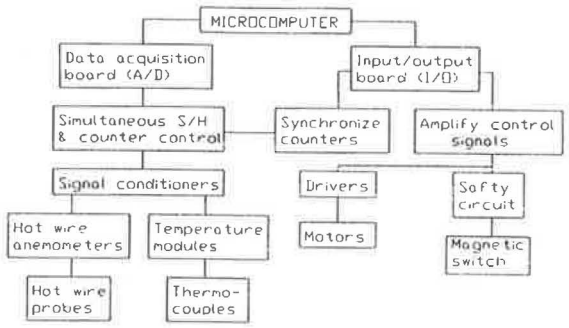

Figure 3 *Diagram of the data acquisition and probe-positioning system.*

[1]The numerical form of the data presented in this paper can be found in Zhang (1991).

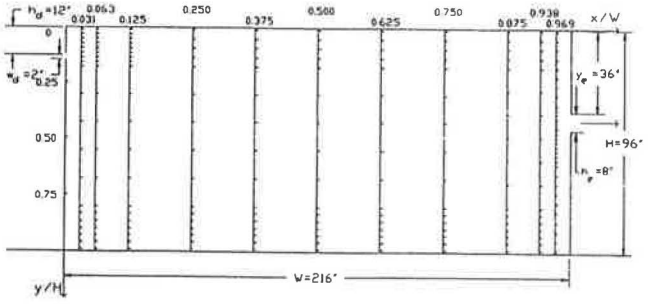

Figure 4 *Probe locations for velocity and temperature measurements.*

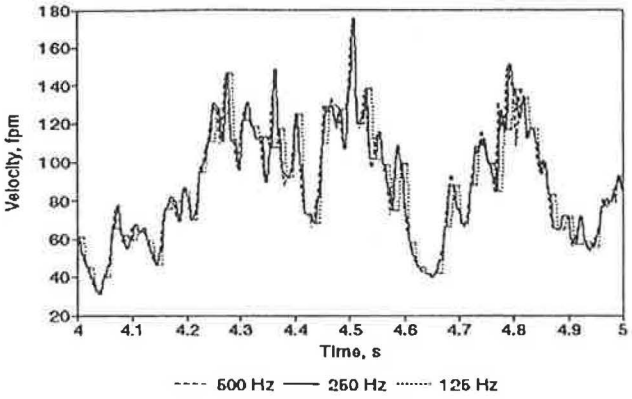

Figure 5 *Effects of sampling rates on the velocity measurements.*

distribution of velocity fluctuations up to 125 Hz. An assumption implied is that velocity fluctuations with frequencies higher than 125 Hz have negligible kinetic energy, which is confirmed by the energy spectrum analysis in this paper.

The sampling period of velocity measurements needs to be long enough to ensure accurate time averages of velocity and turbulent kinetic energy. Figure 6 shows that the mean velocity and turbulent kinetic energy become stable when the sampling period is longer than 15 seconds. It is noted that a longer sampling period is needed to obtain a stable time average for the turbulent kinetic energy than for the velocity.

For the data presented in this paper, a sampling period of 16.384 seconds and a sampling rate of 250 Hz were used, which resulted in 4,096 data points for each of the 205 locations measured.

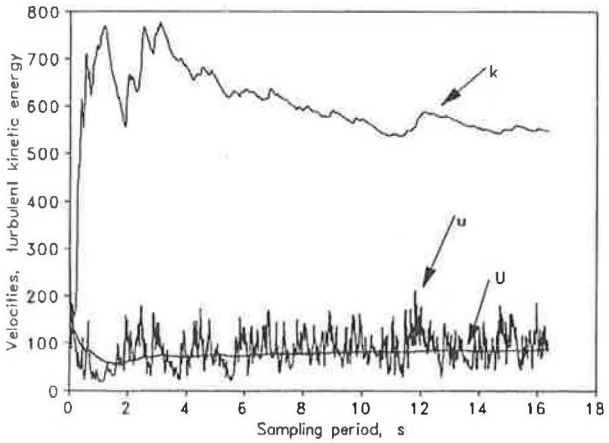

Figure 6 *Effects of sampling periods on the measurements of velocity and turbulent kinetic energy.* u = *instant velocity, ft/min;* U = *time average velocity, ft/min;* k = *turbulent kinetic energy,* $(ft/min)^2$.

Flow Pattern

As shown in Figures 7 and 8, the common flow behavior was that the incoming air attached to the ceiling after entering the room. This is due to the Coanda effect, in which the pressure difference between the two sides of the air jet lifted the jet toward the ceiling. The air then traveled along the ceiling for a certain distance (called attachment length) until it separated from the ceiling or reached the opposite wall. Air below the jet was entrained by the jet so that a reverse flow pattern formed below the jet.

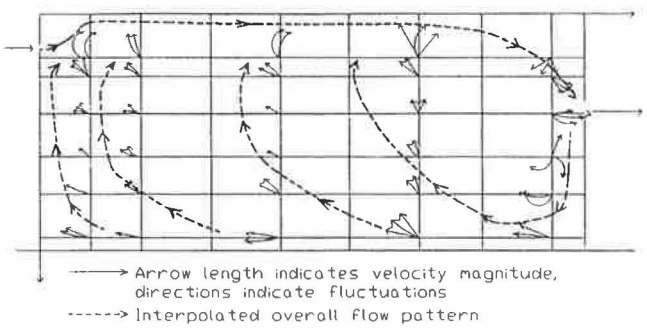

Figure 7 *Airflow pattern for test 1 (isothermal flow).*

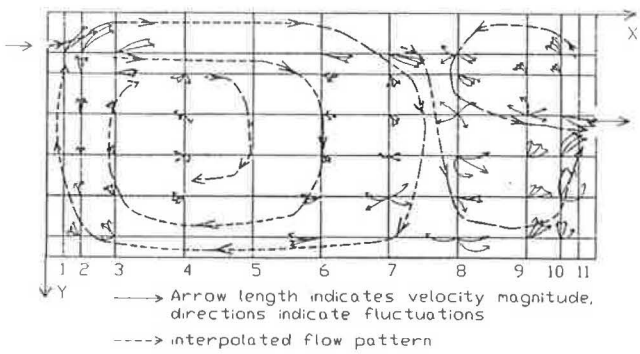

Figure 8 *Airflow pattern for test 2 (non-isothermal flow).*

However, there were substantial differences between the isothermal and non-isothermal tests. In the non-isothermal test, the diffuser jet dropped midway before it reached the opposite wall. This was expected because the incoming air had a lower temperature than the room air. The separation point of the diffuser air jet from the ceiling depends on the balance between the Coanda effect (or inertial effect) and the thermal buoyancy effect.

It was also observed that the airflow in the non-isothermal cases had stronger random behavior, as suggested by the multiple directions of the smoke movement observed at the same location but at different times, compared to the isothermal cases.

Velocity Characteristics at the Diffuser

The mean velocity profile at the diffuser is not uniform (Figure 9). Neither is the turbulent kinetic energy. Numerical modelers usually assume a uniform turbulence intensity between 4% and 5% (e.g., Nielsen 1990; Murakami 1991). This would be appropriate only for the central part of the diffuser. The measured profile of turbulence intensity showed higher values (up to 75%) at the edges of the diffuser opening. Therefore, measured profiles of mean velocity and turbulence intensity at the diffuser are essential for evaluating numerical simulation models of room air distribution.

Spatial Distribution of Mean Velocity

Figures 10 and 11 present the spatial distributions of mean velocity in which all velocities throughout the room are made dimensionless by expressing them as a ratio to the diffuser air velocity. The trajectory of the diffuser jet can be traced by following the locations at which the maximum velocity occurred in each measurement column (x/W). A common feature of the two tests is that the incoming air jet bends toward the ceiling after entering the room. It then travels along the ceiling for a certain distance before separating from the ceiling again.

In the region where the jet attached to the ceiling, the measured velocity profiles are similar to a "wall jet" type flow. The conventional "wall jet" theory (e.g., Schlichting 1979) may be tested with the present data to determine their applicability in describing this region or if

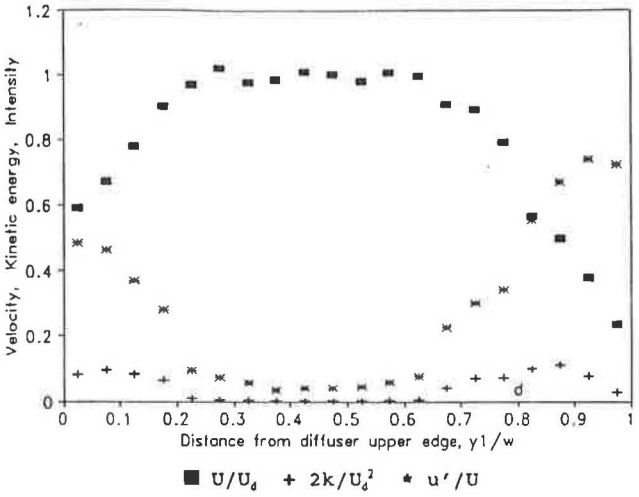

Figure 9 *Mean velocity* (U/U_d), *turbulent kinetic energy* ($2k/U_d^2$), *and turbulence intensity* (u'/U) *at the diffuser.*

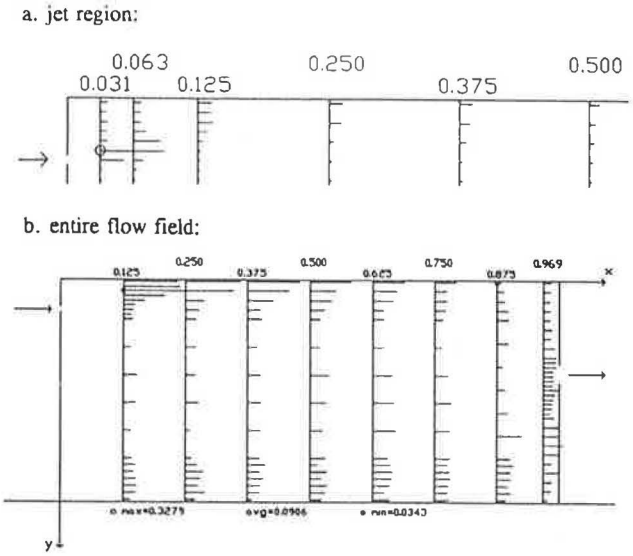

Figure 10 *Distribution of mean velocity* (U/U_d) *for test 1:* U_d *= 350 ft/min,* ΔT_{fd} *= 0 (cross sections of the horizontal and vertical lines represent measured locations; length of a horizontal line represents magnitude).*

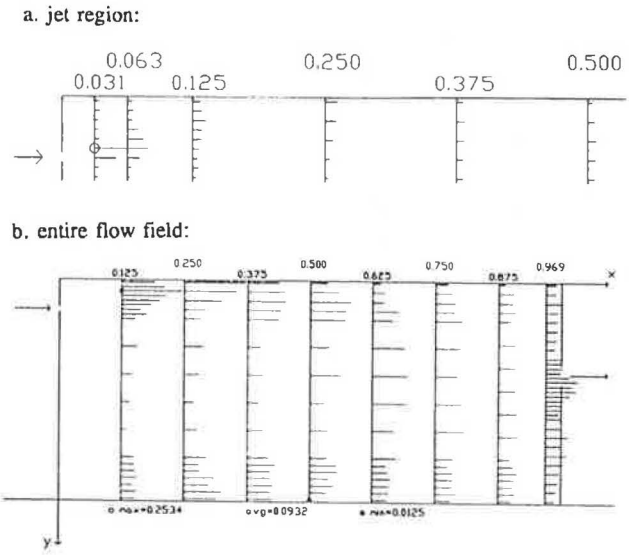

Figure 11 *Distribution of mean velocity* (U/U_d) *for test 2:* U_d *= 350 ft/min,* ΔT_{fd} *= 67.3°F (cross sections of the horizontal and vertical lines represent measured locations; length of a horizontal line represents magnitude).*

modification is necessary for a better prediction.

Comparing the measured velocity distributions to the flow patterns (Figures 7 and 8), one can see that relatively small velocities are present toward the central region of the large recirculation eddy, similar to the velocity distribution along the radius of a rotating body. Timmons (1979) assumed such flow behavior in his inviscid vorticity model. His model predicted well the general airflow patterns, although the average error in predicting the room air velocities was 22%, excluding the regions close to wall surfaces.

The velocity profiles close to the floor ($y/H > .75$) are not similar to the "wall jet" type of flow but are more or less uniform (Figures 10 and 11). With a higher diffuser air velocity (i.e., a higher Re_d than the case studied, a higher remaining momentum from the diffuser air jet would be available to the recirculation flow. Due to the surface effect, a "wall jet" type of flow would also be produced over the floor, as reported by Jin and Ogilvie (1990). This is an important difference between high and low ventilation rate flows (i.e., between high and low Re_d).

The thermal buoyancy decreases the distance at which the air jet travels along the ceiling and also makes the jet expand faster (Figure 10 vs. 11). When the jet falls, it produces a region with relatively high air velocities (x/W = 0.5, 0.625, 0.75 in Figure 11) compared to the other parts of the occupied region. The average velocity in the occupied region is a little higher in the non-isothermal case than in the isothermal case (U/U_d = 0.077 vs. 0.071) since the diffuser air jet drops to the occupied region directly before it is sufficiently mixed with the room air. This type of diffuser jet may cause a "cold draft" and therefore should be avoided in design practice.

Spatial Distribution of Turbulence Intensity

The turbulence intensity is defined as the ratio between the standard deviation (u') of velocity fluctuations and the mean velocity (U). It represents the degree of turbulence at a local point.

The distribution pattern of the turbulence intensity (Figures 12 and 13) within the test room was not as apparent as in the mean velocity distribution. In general, relatively high values were distributed in the intermittent region at the edge of the diffuser air jet and at the central region of the recirculation eddy.

The average turbulence intensity in the occupied region was higher in the non-isothermal test than the isothermal test (29.9% vs. 23.6%), indicating that the thermal buoyancy contributed to the generation of turbulence.

Spatial Distribution of Turbulent Kinetic Energy

The kinetic energy of turbulence (k) is defined as $0.5u'^2$. It is a more appropriate term than the turbulence intensity to represent the importance of turbulence effect on the room air motion because the latter only describes the degree of turbulence locally (Zhang 1991). As shown in Figures 14 and 15, the kinetic energy of turbulence in the diffuser jet region is substantially larger than in the

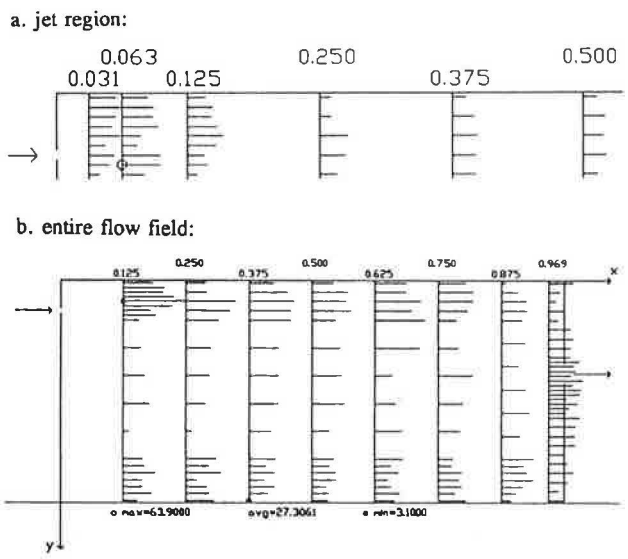

Figure 12 Distribution of turbulence intensity ($100u'/U_d$) for test 1: U_d = 350 ft/min, ΔT_{fi} = 0 (cross sections of the horizontal and vertical lines represent measured locations; length of a horizontal line represents magnitude).

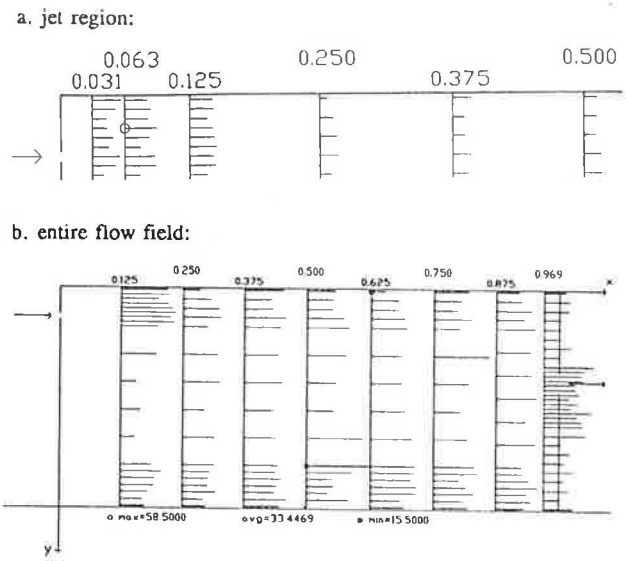

Figure 13 Distribution of turbulence intensity (u'/U_d) for test 2: U_d = 350 ft/min, ΔT_{fi} = 67.3 °F (cross sections of the horizontal and vertical lines represent measured locations; length of a horizontal line represents magnitude).

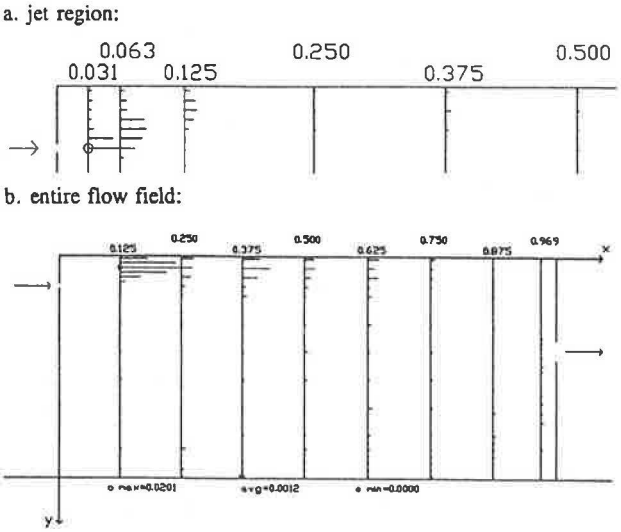

Figure 14 Distribution of turbulent kinetic energy $(k/0.5U_d^2)$ *for test 1:* $U_d = 350$ *ft/min,* $\Delta T_{fi} = 0$ *(cross sections of the horizontal and vertical lines represent measured locations; length of a horizontal line represents magnitude).*

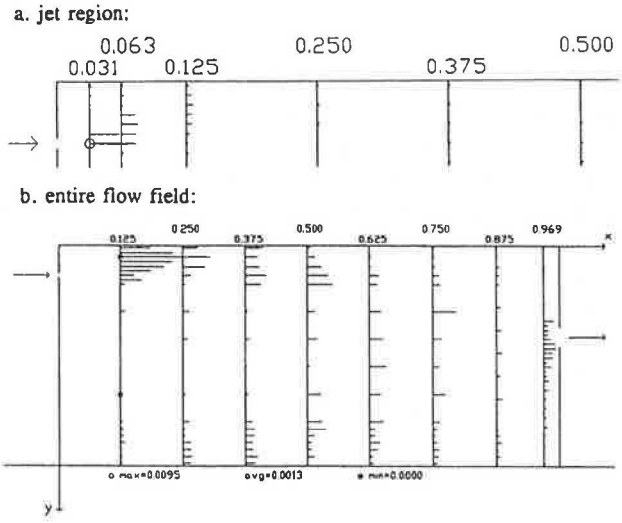

Figure 15 Distribution of turbulent kinetic energy $(k/0.5U_d^2)$ *for test 2:* $U_d = 350$ *ft/min,* $\Delta T_{fi} = 67.3$ *°F.*

occupied region, especially in the isothermal test. Since the magnitude of turbulent kinetic energy in a local region depends on the turbulence generated within the region and that transported from the upstream, one may infer that the turbulence within the room is mainly generated in the diffuser jet region, due to the strong interaction between the incoming air and the room air, and between the jet and the ceiling surface. The generated turbulence is then transported to the other parts of the room. In the transport process, the velocity fluctuations are also damped by the viscous effect, resulting in low turbulent kinetic energy in the occupied region. This phenomenon agrees with the turbulence theory (Hinze 1975), since large mean velocity gradients were present in the jet region but not in the occupied region.

The average turbulent kinetic energy of the occupied region in the non-isothermal flow is approximately 130% larger than in the isothermal flow in this study. This is again due to the contribution of thermal buoyancy to the turbulence production, especially within the occupied region itself.

Spatial Distribution of Mean Temperature

The distribution of mean temperature for the non-isothermal test in this study is mainly determined by the air movement (Figure 16). As the incoming air travels within the room, it is heated by the adjacent warmer air through turbulent mixing and molecular diffusion. However, the room air temperatures in the occupied region are much more uniform than the mean velocity distribution. Therefore, the heat diffuses (which relates to temperature) much faster than the momentum (which relates to velocity) in the room airflows. This is expected since the temperature field has different boundary conditions, and, additionally, the Prandtl number of the air is about 0.7, which represents the ratio between the momentum and thermal diffusion rates (Kays and Crawford 1980).

Energy Spectral Density Function The energy spectral density function $E(f)$ is defined as

$$\int_0^{+\infty} E(f)\,df = (u')^2$$

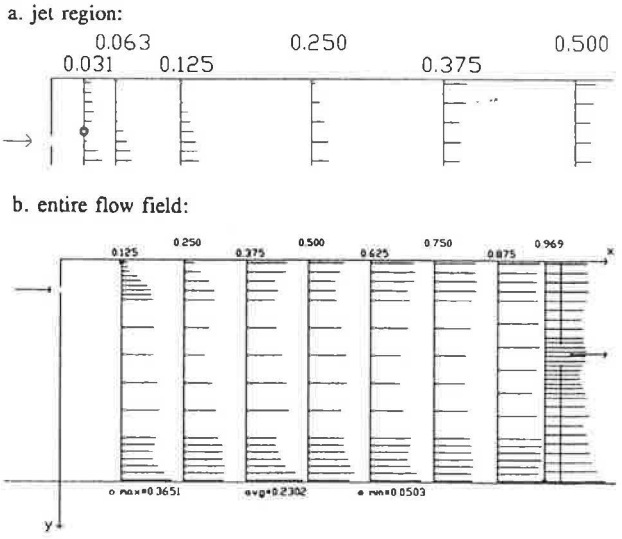

Figure 16 Distribution of temperature $[(T - T_d)/\Delta T_{fi}]$ *for test 2:* $U_d = 350$ *ft/min,* $\Delta T_{fi} = 67.3$ *°F.*

where $(u')^2$ is the variance representing the total energy of the velocity fluctuation. $E(f)$ represents the distribution of the kinetic energy of turbulence fluctuations over different frequency components. The higher frequency components correspond to smaller eddies and the lower to larger eddies.

As shown in Figures 17 and 18, velocities in the jet region contain higher levels of kinetic energy of turbulence compared to the occupied regions. The distribution also extends to higher frequencies for the jet regions. The large velocity gradients in the jet regions are mainly responsible for the generation of the turbulence according to the turbulence theory (Hinze 1975). High-velocity gradients also generate more small eddies that correspond to the high-frequency fluctuations.

Comparing Figure 16 with Figure 17, one can see that thermal buoyancy due to the heat production from the floor increases the kinetic energy of turbulence and also extends the energy spectrum to a higher frequency. This is especially apparent for the occupied regions. Therefore, the thermal buoyancy did contribute to the production of turbulence within the room.

In the high-frequency range, the decay rate of the energy density functions is close to $f^{-5/3}$, similar to that in the isotropic turbulence (Hinze 1975). The energy contained by the velocity fluctuation components with frequencies higher than 100 Hz is negligible.

SUMMARY AND CONCLUSIONS

Detailed experimental data are presented for isothermal and non-isothermal room ventilation flows. These data are useful for evaluating existing numerical simulation models of room air motion. Additionally, the following can be concluded from the above discussions:

1. The turbulence of the room ventilation flows is mainly generated by the diffuser air jet. The turbulent kinetic energy in the occupied region is much smaller and is distributed in a lower frequency range than the diffuser jet region.
2. The internal heat load causes the diffuser air jet to fall earlier, resulting in a higher spatial average of mean velocity in the occupied region compared to the isothermal case with the same diffuser air velocity. Internal heat also contributes to the turbulence production within the room and thereby increases the turbulent kinetic energy and turbulence intensity in the occupied region.
3. The measured velocity and turbulent kinetic energy profiles at the diffuser are nonuniform. The measured turbulence intensity at the diffuser edges is significantly higher than 4% to 5%, as assumed in many numerical simulations of room air motion.

NOMENCLATURE

Ar_{fd} = Archimedes number, defined as

$$\mathrm{Ar}_{fd} = \frac{\beta g \Delta T_{fd}}{U_d^2}$$

$E(f)$ = energy spectrum density of velocity fluctuations, $(\mathrm{ft/min})^2$

f = frequency, Hz

H = height of the room, 8 ft

k = kinetic energy of turbulence, defined as $0.5(u')^2$, $(\mathrm{ft/min})^2$

Q = ventilation rate, ach (air changes per hour)

Re_d = diffuser Reynolds number, defined as

$$\mathrm{Re}_d = \frac{U_d w_d}{\nu}$$

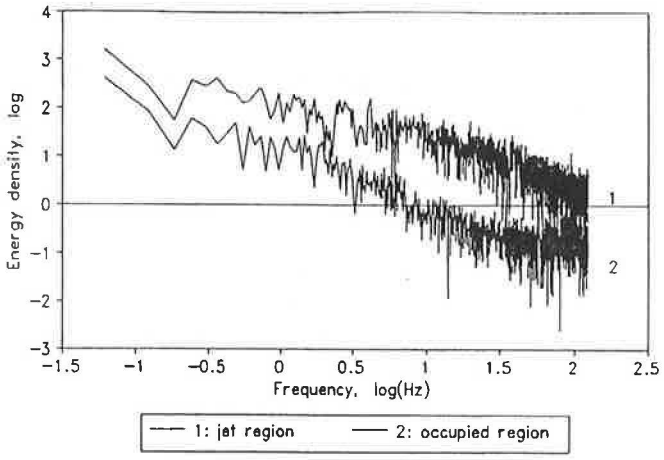

Figure 17 Energy spectrums of velocity signals in test 1: U_d = 350 ft/min, ΔT_{fd} = 0 (jet region: x/W = 0.125, y/H = 0.0521; occupied region: x/W = 0.375, y/H = 0.6771).

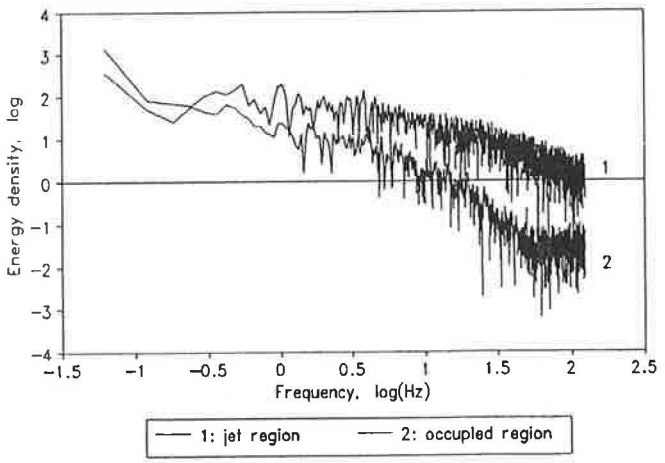

Figure 18 Energy spectrums of velocity signals in test 2: U_d = 350 ft/min, ΔT_{fd} = 67.3°F (jet region: x/W = 0.125, y/H = 0.0521; occupied region: x/W = 0.375, y/H = 0.6771).

T	=	mean temperature at a measured location, °F
T_d	=	temperature at the diffuser, °F
T_e	=	temperature at the exhaust, °F
T_f	=	temperature at the floor surface, °F
U	=	mean velocity at a measured location, ft/min
U_d	=	mean velocity at the center of the diffuser opening, ft/min
u'	=	standard deviation of velocity, ft/min
W	=	width of the room, 18 ft
w_d	=	width of the slot diffuser, 2 in.
x	=	horizontal coordinate
y	=	vertical coordinate
$y1$	=	distance from the upper edge of the diffuser slot
ΔT_{fd}	=	temperature difference between the floor surface and the diffuser air

ACKNOWLEDGMENT

This study was sponsored by the U.S. National Science Foundation and the University of Illinois Campus Research Board. Their financial support is highly appreciated.

REFERENCES

ASHRAE. 1989. *Fundamentals*. ASHRAE Handbook. Atlanta, GA: American Society of Heating, Refrigerating, and Air-Conditioning Engineers, Inc.

Bendat, J.S., and A.G. Piersol. 1986. *Random data—Analysis and measurement procedures*. New York: John Wiley & Sons.

Christianson, L.L., ed. 1989. *Building systems: Room air and air contaminant distribution*. Atlanta: American Society of Heating, Refrigerating, and Air-Conditioning Engineers, Inc.

Hanzawa, H., A.K. Melikow and P.O. Fanger. 1987. Airflow characteristics in the occupied zone of ventilated spaces. *ASHRAE Transactions* 93(1): 524-539.

Hart, G.H., and D. Int-Hout. 1980. The performance of a continuous linear air diffuser in the perimeter zone of an office environment. *ASHRAE Transactions* 86(2): 107-124.

Hinze, J.O. 1975. *Turbulence*. New York: McGraw-Hill Book Co.

Jin, Y., and J.R. Ogilvie. 1990. Near floor air speeds from center slot air inlets in swine barns. ASAE Paper No. 904004. St. Joseph, MI: American Society of Agricultural Engineers.

Kays, W.M. and M.E. Crawford. 1980. *Convective heat and mass transfer*. New York, NY: McGraw-Hill, Inc.

Lorch, F.A., and H.E. Straub. 1983. Performance of overhead slot diffusers with simulated heating and cooling conditions. *ASHRAE Transactions* 89(1B): 200-211.

Miller, P.L., and R.T. Nash. 1971. A further analysis of room air distribution performance. *ASHRAE Transactions* 77(2): 205.

Murakami, S. 1991. Numerical prediction of horizontal non-isothermal 3-D jet in room based on the k-ϵ model. *ASHRAE Transactions* 97(1).

Murakami, S., and S. Kato. 1989. Current status of numerical and experimental methods for analyzing flow field and diffusion in a room. In: *Building Systems: Room Air and Air Contaminant Distribution*, ed. L.L. Christianson. Atlanta: American Society of Heating, Refrigerating, and Air-Conditioning Engineers, Inc.

Nielsen, P.V. 1989. Numerical prediction of air distribution in rooms—Status and potentials. In: *Building Systems: Room Air and Air Contaminant Distribution*, ed., L.L. Christianson. Atlanta: American Society of Heating, Refrigerating, and Air-Conditioning Engineers, Inc.

Nielsen, P.V. 1990. Specification of a two-dimensional test case. Internal report for IEA Annex 20: Air Flow Pattern within Buildings. University of Aalborg. ISSN 0902-7513 R9040.

Sandberg, M. 1989. Velocity characteristics in mechanically ventilated office rooms. RoomVent '87, June. Stockholm, Sweden, Session 2A.

Schliching, H. 1979. *Boundary-layer theory*. New York, NY: McGraw-Hill, Inc.

Straub, H.E., and M.M. Chen. 1957. Distribution of air within a room for year-round air conditioning—Part II. *University of Illinois Engineering Experiment Station Bulletin*, No. 442.

Timmons, M.B. 1979. Experimental and numerical study of air movement in slot-ventilated enclosures. Unpublished Ph.D. thesis, Cornell University Libraries, Ithaca, NY.

Wu, G.J., L.L. Christianson, J.S. Zhang, and G.L. Riskowski. 1990. Adjustable room ventilation simulator for room air and air contaminant distribution modeling. *Indoor Air '90*. Proceedings of the Fifth International Conference on Indoor Air Quality and Climate, Vol. 4, pp. 237-242.

Zhang, J.S. 1991. A fundamental study of two-dimensional room ventilation flows under isothermal and non-isothermal conditions. Unpublished Ph.D. thesis, University of Illinois at Urbana-Champaign.

Zhang, J.S., L.L. Christianson, and G.L. Riskowski. 1989. Regional airflow characteristics in a mechanically ventilated room under non-isothermal conditions. *ASHRAE Transactions* 95(2).